THIS IS AN EARLIER VERSION OF THE PAPER WITH DOI: 10.1109/LMWC.2018.2862646

A G-band Broadband Balanced Power Amplifier Module Based on Cascode mHEMTs

B. Amado-Rey, Y. Campos-Roca, C. Friesicke, F. van Raay, H. Massler, A. Leuther, and O. Ambacher

***Abstract*—The first full G-band power amplifier module demonstrated in GaAs metamorphic high electron mobility transistor (mHEMT) technology has been developed for use as a driver amplifier in instrumentation. The circuit integrated in this module uses a compact balanced cascode topology and is based on a 35 nm mHEMT technology in a grounded coplanar waveguide (GCPW) environment. High compactness is achieved due to the use of a small ground-to-ground spacing of $14\ \mu m$ and an advanced process with three metallization layers. The MMIC exhibits a linear gain higher than $15.3\ dB$ and return losses better than $10\ dB$ from 118 to $236\ GHz$, which represents an ultra broad relative bandwidth (RBW) of $67\,\%$. A peak output power of $10\ dBm$ is achieved at $200\ GHz$. The WR-5 module uses broadband transitions, which show insertion losses of less than $1.5\ dB$. It demonstrates a small-signal gain that exceeds $13.4\ dB$ in the whole G-band (RBW$\geq$ $54\ \%$). Large signal characterization exhibits power levels higher than $3.6\ dBm$ from 130 to $210\ GHz$ (RBW=$47\ \%$). This module achieves the highest bandwidth in G-band and the highest output power when comparing it with modules based on similar technologies.**

***Index Terms*—Monolithic millimeter-wave integrated circuit (MMIC), balanced power amplifier, grounded coplanar waveguide (GCPW), G-band, WR-5, module.**

I. INTRODUCTION

THE G-BAND (140-220 GHz) frequency range offers interesting possibilities for high data-rate wireless communication systems as well as high-resolution imaging and sensing. Medium power amplifiers (MPAs) are demanded for these systems and their implementation through a monolithic millimeter-wave integrated circuit (MMIC) solution provides advantages in terms of compactness and performance.

Packaging MMICs into modules is necessary for connecting the diverse components that constitute the final system. Also, one possibility to overcome the low transistor breakdown voltage issues that limit the available output power at millimeter-wave frequencies is to combine many modules in parallel. In [1] a state-of-the-art G-band 16-way module is demonstrated, which exhibits an output power of $820\,\mathrm{mW}$ and is based on InP HBTs. Single modules in InP HEMT and GaAs metamorphic HEMT (mHEMT) technologies are also investigated in [2] and [3], respectively. The module presented in this paper is used as driver for instrumentation, due to the limited power available in the measurement system.

To the authors' knowledge, the first full G-band MPA module in GaAs mHEMT technology is presented in this paper, which shows an ultra-broad small- and large-signal relative bandwidths (RBWs) of $54\,\%$ and $47\,\%$, respectively, with output power exceeding $3.6\,\mathrm{dBm}$.

II. TECHNOLOGY

The MMIC integrated in the G-band module was fabricated using a 35 nm mHEMT process on GaAs, with an $In_{0.52}Al_{0.48}As/In_{0.80}Ga_{0.20}As$ single channel technology. The active devices consist of T-shaped 35 nm Pt-Ti-Pt-Au gates, which are defined by e-beam lithography. For a $2 \times 10\,\mu\mathrm{m}$ device, a maximum channel current of $1600\,\mathrm{mA/mm}$ is achieved [4]. A transit frequency of $550\,\mathrm{GHz}$ and a maximum oscillation frequency above $1\,\mathrm{THz}$ are measured for the same device geometry. On- and off-state breakdown voltages values are $1.5\,\mathrm{V}$ and $2\,\mathrm{V}$, respectively.

A new in-house process, based on three metallization layers, has recently been introduced [4]. Instead of the in-house established two-layer process, this one is characterized by the use of three metal layers (two evaporated $0.3\,\mu\mathrm{m}$-Au layers, and a galvanic $2.7\,\mu\mathrm{m}$-thick plated Au metallization, which is also available in air-bridge technology). This process includes two benzocyclobutene (BCB) layers, the first of which is deposited on the substrate and has a thickness of $0.3\,\mu\mathrm{m}$. The second additional $1.4\,\mu\mathrm{m}$ BCB layer is placed between the two $0.3\,\mu\mathrm{m}$ Au layers. By reducing the SiN thickness to $80\,\mathrm{nm}$, compact metal-insulator-metal (MIM) capacitors are provided.

The grounded coplanar waveguide (GCPW) lines have a ground-to-ground (G2G) spacing of $14\,\mu\mathrm{m}$. After front side processing, the GaAs substrate is thinned down to $50\,\mu\mathrm{m}$ and one backside $2.7\,\mu\mathrm{m}$-thick plated Au layer was deposited on the wafer backside. Through substrate via-holes are realized to contact the top-bottom ground planes in the GCPW for the suppression of substrate resonances.

III. MMIC DESIGN AND EXPERIMENTAL RESULTS

Apart from the good broadband return losses (RLs) and the improvement of output power, balanced amplifiers are much more stable than their single counterparts. That is due to the improvement of the odd-mode stability between branches.

In Fig. 1 (a) the balanced configuration used for the MMIC is shown. Tandem couplers with a measured insertion loss (IL) of less than $1.3\,\mathrm{dB}$ per coupler are used as 90° hybrids. The paralleled single cells consist of two cascode stages with $4 \times 8\,\mu\mathrm{m}$ and $4 \times 12\,\mu\mathrm{m}$ device geometries. The selection of the cascode configuration is due to the higher

B. Amado-Rey is with the Institute for Microsystem Techniques, Albert-Ludwigs-University, Freiburg, Germany. E-mail: aamadore@alumnos.unex.es

F. van Raay, H. Massler, C. Friesicke, A. Leuther, and O. Ambacher are with the Fraunhofer IAF, Freiburg 79108, Germany

Y. Campos-Roca is with the Department of Computer and Communication Technologies, University of Extremadura, Caceres 10003, Spain.

Manuscript received XXXX XX, XXXX; revised XXXX XX, XXXX.

gain and wider bandwidth (because of Miller's effect) than the common-source (CS) configuration by itself. Each cascode stage has been modeled by using a series connection of a CS and a common-gate (CG) in-house analytic transistor models. In between, a 14 µm G2G GCPW line model is used (see Fig. 1 (b)). This cascode model has been experimentally verified up to 330 GHz.

To even further enhance the bandwidth, the matching network (MN) between the two cascode stages is built by using a third-order broadband approach based on two shorted and open stubs, which are separated by GCPW lines and a series DC blocking capacitor C_{IS}, as shown in Fig. 1 (b).

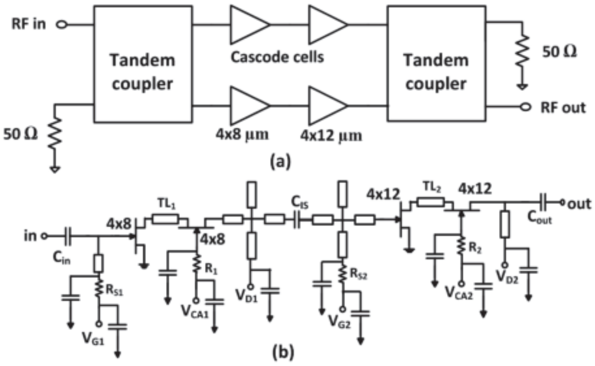

Fig. 1. Block diagram of (a) the designed balanced PA configuration and (b) the cascode cells.

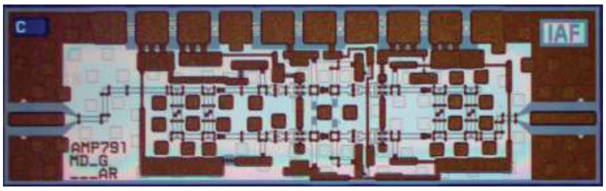

Fig. 2. Chip photo of the cascode MPA MMIC. Size: $1.5 \times 0.5\,\mathrm{mm}^2$.

The chip photograph of the G-band balanced MPA is shown in Fig. 2. As shown, the chip is very compact. S-parameter measurements of this MMIC are illustrated in Fig. 3. The on-wafer measured and simulated results present a good agreement. Two peak small-signal gain values of 22.7 dB and 22.4 dB are obtained at 126 and 240 GHz, respectively. The measurements exhibit a gain higher than 15.3 dB, and RLs better than 10 dB from 118 GHz to 236 GHz. This is equivalent to an ultra-broad RBW of 67 %, which is a result of the following factors: the low losses of the implemented matching networks (MNs), the third-order MN between the two stages, the reduction of the Miller's effect from the cascode configuration and the balanced MPA topology.

The on-wafer large-signal gain and output power frequency sweeps are shown in Fig. 4, for two different input power levels: $P_{in} = -11\,\mathrm{dBm}$ and $P_{in}=-6\,\mathrm{dBm}$. To be consistent, the bias conditions applied are the same as for the small-signal measurements. At $P_{in} = -11\,\mathrm{dBm}$, peak gain and output power of 21.4 dB and 10.4 dBm, respectively, occur at 130 GHz. When applying a higher input power level ($P_{in}=-6\,\mathrm{dBm}$) the output power increases, with a peak value of 10 dBm at 200 GHz. Higher output power values than 9 dBm are measured from 170 to 200 GHz (16 %), and the compressed gain in this range exceeds 15 dB. Furthermore, output power levels exceeding 6.2 dBm are measured from 130 to 230 GHz (56 % of large-signal RBW). Thus, results of CS amplifiers (with $P_{out} = 7.4\,\mathrm{dBm}$ at 200 GHz and RBW of 13 % in [5]) are overcome when using the cascode configuration.

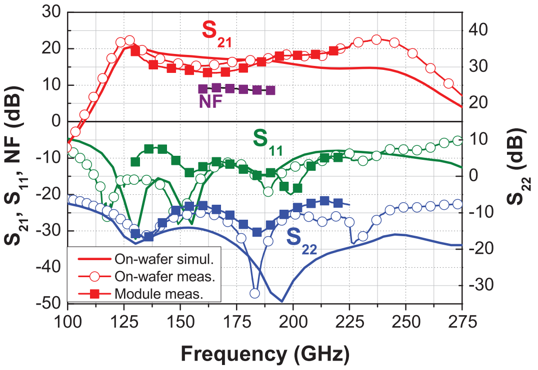

Fig. 3. Measured and simulated S-parameters of the broadband MPA MMIC. On-wafer bias: $V_{G1} = V_{G2} = 0.134\,\mathrm{V}$; $V_{CA1} = V_{CA2} = 1.134\,\mathrm{V}$; $V_{D1} = V_{D2} = 2\,\mathrm{V}$, $I_D = 300\,\mathrm{mA/mm}$. Module bias: $V_{G1} = V_{G2} = 0.2\,\mathrm{V}$; $V_{CA1} = V_{CA2} = 1.2\,\mathrm{V}$; $V_{D1} = V_{D2} = 2.0\,\mathrm{V}$ and $I_D = 344\,\mathrm{mA/mm}$.

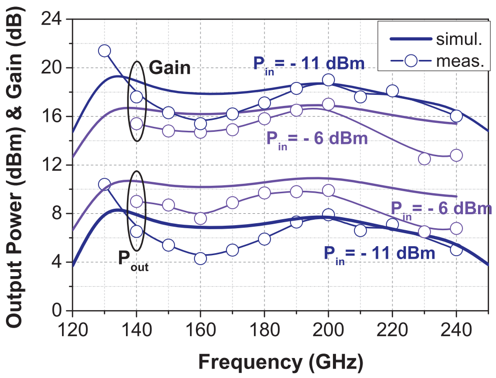

Fig. 4. On-wafer MMIC large-signal results. $V_{G1} = V_{G2} = 0.134\,\mathrm{V}$; $V_{CA1} = V_{CA2} = 1.134\,\mathrm{V}$;$V_{D1} = V_{D2} = 2\,\mathrm{V}$ and $I_D = 300\,\mathrm{mA/mm}$.

IV. G-BAND MODULE AND EXPERIMENTAL RESULTS

The MMIC was packaged in a WR-5 waveguide housing. In Fig. 5(a), the interior of the module is plotted which includes the processed power amplifier chip, the transition E-plane probes and the DC interconnection. The probe transitions have been realized on 50 µm thick quartz substrates and are connected to the chip through 17 µm wirebond lines. The ILs of the transitions are less than 1.5 dB from 140 to 220 GHz for a single transition [6]. The final module is shown in Fig. 5(b).

Fig. 3 illustrates the measured S-parameters and the noise factor (NF) of the WR-5 module. It achieves a small-signal gain of more than 13.4 dB from 130 to 230 GHz, with a peak of 20.6 dB at 225 GHz. It demonstrates a best noise figure (NF) value of 8.59 dB (1806 K) at 190 GHz.

The large-signal module characterization is shown in Fig. 6. At $P_{in}=-6\,\mathrm{dBm}$, output power and gain higher than 2.6 dBm

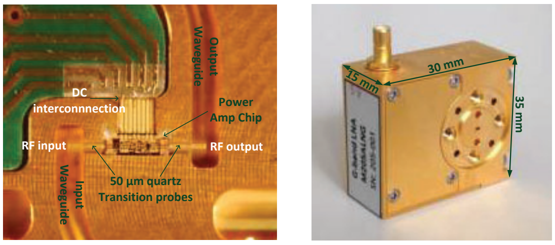

Fig. 5. (a) Inner view of the mounted MMIC MPA and (b) photograph of the G-band final module with a size of $30 \times 35 \times 15\,\mathrm{mm}^3$.

and $8.6\,\mathrm{dB}$, respectively, are achieved from 130 to 210 GHz. When increasing the input power level, the output power is simultaneously increased, exceeding $3.6\,\mathrm{dBm}$ from 150 to 190 GHz at P_{in}=$-4\,\mathrm{dBm}$. A peak output power level of $5.6\,\mathrm{dBm}$ is obtained at 190 GHz, with a corresponding power added efficiency of $1.5\,\%$. The difference with the on-wafer power measurements is mainly due to the insertion loss of the transition and the different bias point applied.

At 130-140 GHz and 200-210 GHz only lower input power levels are measured due to the limited input power of the system at these frequencies. Anyway the $3.6\,\mathrm{dBm}$ level of output power is also overcome. Hence the large signal RBW is extended from 130 to 210 GHz (47 %).

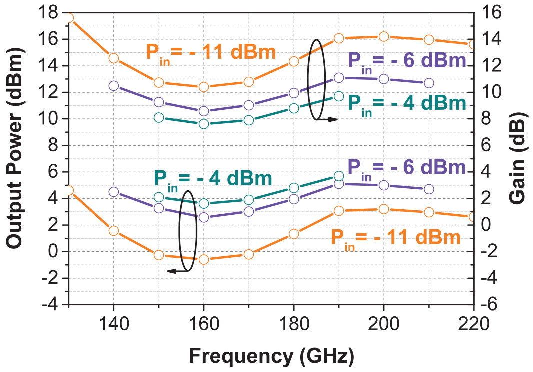

Fig. 6. Large-signal module measurements. DC biasing: V_{G1}=V_{G2}=0.2 V; V_{CA1}=V_{CA2}=1.2 V; V_{D1}=V_{D2}=2.0 V and $I_D = 344\,\mathrm{mA/mm}$.

V. DISCUSSION

A comparison of the performance of this G-band waveguide module with the state-of-the art modules in similar frequency ranges is included in Tab. I. The highest output power, which exceeds $18\,\mathrm{dBm}$ from 190 to 228 GHz (18 % of large-signal RBW) is achieved by [1]. This performance is obtained when using a $250\,\mathrm{nm}$ InP HBT technology, which has a higher breakdown voltage than the GaAs mHEMT technology. A similar case regarding the high breakdown voltage is [2].

However, within the same technology, the output power bandwidth of the amplifier in [3] is considerably enhanced in the realized module, whose output power is higher than $3.6\,\mathrm{dBm}$ for 47 % of large-signal bandwidth. Besides that, the small-signal RBW is extremely large (54 %) and better than the other modules included in Tab. I. The on-wafer results achieved a wider bandwidth, but the package is built to operate only within the G-band range.

TABLE I
COMPARISON OF POWER AMPLIFIER MODULES AROUND G-BAND.

Gate length Technology	250 nm InP HBT	sub-50 nm InP HEMT	35 nm mHEMT	35 nm mHEMT
LS RBW$^+$	190.8-228 (18 %)	205-225 (9 %)	275-320 (15 %)	130-210 (47 %)
P_{out} **(dBm)**	> 18	> 18	> 2.7	> 3.6
Linear gain (dB)	> 14	> 16	> 15	> 13.4
S_{21} **RBW**	205-247 (19 %)	205-225 (9 %)	220-320 (37 %)	130-225 (54 %)
3-dB bandwidth (small-signal)	205-247 (19 %)	205-225 (9 %)	240-224 (6.1 %) 275-305 (10.3 %)	> 130-134 (> 3 %) > 191-225 (> 16.3 %)
FET $V_{d,DC}(V)$	2.2	2	0.9	1
Transition loss (dB)	1	1.2	1.2	1.5
Reference	[1] *	[2]	[3]	This work

+ This is the RBW referred to the large-signal performance.

* Values are obtained from the MMIC measurements taking into account 1 dB loss per transition (only for one module).

VI. CONCLUSION

This paper demonstrates the first full-coverage G-band MPA module in GaAs mHEMT technology. Linear gain levels higher than $13.4\,\mathrm{dB}$ are exhibited in the whole bandwidth, that corresponds to an ultra-broadband small-signal performance of $54\,\%$, which overcomes the state-of-the art results. The output power exceeds $3.6\,\mathrm{dBm}$ in a $47\,\%$ RBW.

ACKNOWLEDGMENT

The authors would like to thank the IAF Technology Department for the excellent work done during wafer processing.

REFERENCES

[1] J. M. Rollin, D. Miller, M. Urteaga, Z. M. Griffith, and H. Kazemi, “A polystrata 820 mW G-Band solid state power amplifier,” in *2015 IEEE Comp. Semicond. Integr. (CSICS)*, Oct 2015, pp. 1–4.

[2] V. Radisic, K. M. K. H. Leong, S. Sarkozy, X. Mei, W. Yoshida, P. H. Liu, and R. Lai, “A 75 mW 210 GHz power amplifier module,” in *2011 IEEE Comp. Semicond. Integr. (CSICS)*, Oct 2011, pp. 1–4.

[3] A. Tessmann, A. Leuther, V. Hurm, H. Massler, S. Wagner, M. Kuri, M. Zink, M. Riessle, H. P. Stulz, M. Schlechtweg, and O. Ambacher, “A broadband 220-320 GHz medium power amplifier module,” in *2014 IEEE Comp. Semicond. Integr. (CSICS)*, Oct 2014, pp. 1–4.

[4] R. Weber, A. Tessmann, H. Massler, A. Leuther, and U. J. Lewark, “600 GHz resistive mixer S-MMICs with integrated multiplier-by-six in 35 nm mHEMT technology,” in *2016 11th Eur. Microw. Integrat. (EuMIC)*, Oct 2016, pp. 85–88.

[5] I. Kallfass, P. Pahl, H. Massler, A. Leuther, A. Tessmann, S. Koch, and T. Zwick, “A 200 GHz monolithic integrated power amplifier in metamorphic HEMT technology,” *IEEE Microw. Wirel. Co.*, vol. 19, no. 6, pp. 410–412, June 2009.

[6] A. Tessmann, I. Kallfass, A. Leuther, H. Massler, M. Kuri, M. Riessle, M. Zink, R. Sommer, A. Wahlen, H. Essen, V. Hurm, M. Schlechtweg, and O. Ambacher, “Metamorphic HEMT MMICs and modules for use in a high-bandwidth 210 GHz radar,” *IEEE J. Solid-State Circ.*, vol. 43, no. 10, pp. 2194–2205, Oct 2008.